

Gaugino mass non-universality in an $SO(10)$ supersymmetric Grand Unified Theory: low-energy spectra and collider signals

Subhaditya Bhattacharya¹ and Joydeep Chakraborty²

Regional Centre for Accelerator-based Particle Physics

Harish-Chandra Research Institute

Chhatnag Road, Jhansi, Allahabad - 211 019, India

Abstract

We derive the non-universal gaugino mass ratios in a supergravity (SUGRA) framework where the higgs superfields belong to the non-singlet representations **54** and **770** in a $SO(10)$ Grand Unified Theory (GUT). We evaluate the ratios for two intermediate breaking chains, namely, $SU(2) \times SO(7)$ and $SU(4)_C \times SU(2)_L \times SU(2)_R$ (G_{224}) assuming the breaking of the $SO(10)$ GUT group to the intermediate gauge group and that to the Standard Model (SM) takes place at the GUT scale itself. After a full calculation of the gaugino mass ratios, correcting some mistakes in the earlier calculation for 54, we obtain some new interesting low scale phenomenology of such breaking patterns after running down by the renormalization group equations (RGE). We also study the collider signatures in multilepton channels at the Large Hadron Collider (LHC) experiment for some selected benchmark points allowed by the cold dark matter relic density constraint provided by the WMAP data.

¹E-mail: subha@mri.ernet.in

²E-mail: joydeep@mri.ernet.in

1 Introduction

With the Large Hadron Collider (LHC) about to be operative shortly, the search for physics beyond the standard model (SM) has reached a new height of excitement. Low energy (TeV scale) supersymmetry (SUSY) has persistently remained one of the leading candidates among scenarios beyond the Standard Model (SM), not only because of its attractive theoretical framework, but also for the variety of phenomenological implications it offers [1, 2, 3, 4]. The stabilization of the electroweak symmetry breaking (EWSB) scale and the possibility of having a cold dark-matter (CDM) candidate with conserved R -parity ($R = (-1)^{(3B+L+2S)}$) [5] are a few elegant phenomenological features of SUSY. Side by side, the possibility of paving the path towards a Grand Unified Theory (GUT) is one of its most exciting theoretical prospects, where one can relate the $SU(3)$, $SU(2)$ and $U(1)$ gauge couplings and the corresponding gaugino masses at a high-scale [4, 6, 7].

The most popular framework of SUSY-breaking is the minimal supergravity (mSUGRA) scheme, where SUSY is broken in the 'hidden sector' via gravity mediation and as a result, one can parametrize all the SUSY breaking terms by a universal gaugino mass ($M_{1/2}$), a universal scalar mass (m_0), a universal trilinear coupling parameter A_0 , the ratio of the vacuum expectation values (vev) of the two higgses ($\tan\beta$) and the sign of the SUSY-conserving Higgs mass parameter, ($sgn(\mu)$) [4, 8].

However, within the ambits of a SUGRA-inspired GUT scenario itself, one might find some deviations from the above-mentioned simplified and idealized situations mentioned above. For instance, the gaugino mass parameter ($M_{1/2}$) or the common scalar mass parameter (m_0) can become *non-universal* at the GUT scale. In this particular work, we adhere to a situation with non-universal gaugino masses in a supersymmetric scenario embedded in $SO(10)$ GUT group.

Gaugino masses, arising after GUT-breaking and SUSY-breaking at a high scale, crucially depend on the gauge kinetic function, as discussed in the next section. One achieves universal gaugino masses if the hidden sector fields (Higgses, in particular), involved in GUT-breaking, are singlets under the underlying GUT group. However, the inclusion of higher dimensional terms (dimension five, in particular) in the non-trivial expansion of the gauge-kinetic function, where the higgses belonging to the symmetric product of the adjoint representation of the underlying GUT group are non-singlets, makes the gaugino masses M_1 , M_2 and M_3 non-universal at the high scale itself. It is also possible to have more than one GUT representations involved in SUSY breaking, in which case the non-universality arises from a linear combination of the effects mentioned above.

Although this issue has been explored in earlier works, particularly in context of the $SU(5)$ [9, 10, 11], there have been a very few efforts [12] to study the same in context of the $SO(10)$. In this paper, we calculate the non-universal gaugino mass ratios for the non-singlet representations **54** and **770**, based on the results obtained in [13], for two intermediate gauge groups, namely, $SU(2) \times SO(7)$ and the Pati-Salam gauge group $SU(4)_c \times SU(2)_L \times SU(2)_R$ (G_{224}). We also perform a scan over a wide region of parameter space to analyze the low-scale phenomenology of these non-universal gaugino mass ratios at the EWSB scale, after running down by the renormalisation group equation (RGE). We discuss the consistency of such low-energy spectra with radiative electroweak symmetry breaking (REWSB) and other RGE constraints like Landau pole, avoiding tachyonic masses etc. We also point out constraints from stau-LSP, adhering to a situation with conserved R -parity and hence lightest neutralino- LSP, and flavour constraints like $b \rightarrow s\gamma$ for all possible combination of the parameter space points. We then choose some benchmark points consistent with the relic density constraint obtained for cold dark matter [5] from WMAP data [14]. We perform the so-called ‘multilepton channel analysis’ [15, 16] in *same-sign* and *opposite-sign* dileptons, trileptons associated with *jets*, inclusive $4-lepton$ channel as well as in hadronically quiet trilepton channel at these benchmark points. Although there has been a lot of efforts in discussing various phenomenological aspects of such high-scale non-universality and its effect in terms of collider signature [17, 18, 19, 20, 21, 22], our results, which are new given the non-universal ratios, might be important in pointing out the departure in ‘signature-space’ [23, 24, 25, 26, 27, 28, 29] for various choices of gaugino non-universality and possible distinction with the mSUGRA at the LHC.

The paper is organized as follows. In the following section, we calculate the non-universal gaugino mass ratios for the above-mentioned two representations. In section 3, we discuss the low energy spectra obtained for these non-universal ratios in a wide region of parameter space, their consistency and the choice of the benchmark points. Section 4 contains the strategy for collider simulation in context of the LHC at those benchmark points and the numerical results obtained. We conclude in section 5.

2 Non-universal Gaugino mass ratios for $SO(10)$

In this section, we calculate non-universal gaugino mass ratios for non-singlet higgs belonging to representations 54 and 770 under $SO(10)$ SUSY-GUT scenario.

We adhere to a situation where all soft SUSY breaking effects arise via hidden sector interactions in an underlying supergravity (SUGRA) framework, specifically, in $SO(10)$ gauge theories with an arbitrary chiral matter superfield content coupled to N=1 supergravity.

All gauge and matter terms including gaugino masses in the N=1 supergravity lagrangian depend crucially on two fundamental functions of chiral superfields [30]: (i) gauge kinetic function $f_{\alpha\beta}(\Phi)$, which is an analytic function of the left-chiral superfields Φ_i and transforms as a symmetric product of the adjoint representation of the underlying gauge group (α, β being the gauge generator indices); and (ii) $G(\Phi_i, \Phi_i^*)$, a real function of Φ_i and gauge singlet, with $G = K + \ln|W|$ (K is the Kähler potential and W is the superpotential).

The part of the N=1 supergravity lagrangian containing kinetic energy and mass terms for gauginos and gauge bosons (including only terms containing the real part of $f(\Phi)$) reads

$$e^{-1}\mathcal{L} = -\frac{1}{4}Re f_{\alpha\beta}(\phi)(-1/2\bar{\lambda}^\alpha \not{D}\lambda^\beta) - \frac{1}{4}Re f_{\alpha\beta}(\phi)F_{\mu\nu}^\alpha F^{\beta\mu\nu} + \frac{1}{4}e^{-G/2}G^i((G^{-1})_i^j)[\partial f_{\alpha\beta}^*(\phi^*)/\partial\phi^{*j}]\lambda^\alpha\lambda^\beta + h.c \quad (1)$$

where $G^i = \partial G/\partial\phi_i$ and $(G^{-1})_j^i$ is the inverse matrix of $G^j_i \equiv \partial G/\partial\phi^{*i}\partial\phi_j$, λ^α is the gaugino field, and ϕ is the scalar component of the chiral superfield Φ , and $F_{\mu\nu}^\alpha$ is defined in unbroken $SO(10)$. The F -component of Φ enters the last term to generate gaugino masses with a consistent SUSY breaking with non-zero vev of the chosen F . Thus, equation (1) can be rewritten as

$$e^{-1}\mathcal{L} = -\frac{1}{4}Re f_{\alpha\beta}(\phi)(-1/2\bar{\lambda}^\alpha \not{D}\lambda^\beta) - \frac{1}{4}Re f_{\alpha\beta}(\phi)F_{\mu\nu}^\alpha F^{\beta\mu\nu} + \frac{F_{\dot{\alpha}\dot{\beta}}^j}{2}[\partial f_{\alpha\beta}^*(\phi^{*j})/\partial\phi^{*j}_{\dot{\alpha}\dot{\beta}}]\lambda^\alpha\lambda^\beta + h.c \quad (2)$$

where

$$F_{\dot{\alpha}\dot{\beta}}^j = \frac{1}{2}e^{-G/2}[G^i((G^{-1})_i^j)]_{\dot{\alpha}\dot{\beta}} \quad (3)$$

The Φ^j s can be a set of GUT singlet supermultiplets Φ^S , which are part of the hidden sector, or a set of non-singlet ones Φ^N , fields associated with the spontaneous breakdown of the GUT group to $SU(3) \times SU(2) \times U(1)$. The non-trivial gauge kinetic function $f_{\alpha\beta}(\Phi^j)$ can be expanded in terms of the non-singlet components of the chiral superfields in the following way

$$f_{\alpha\beta}(\Phi^j) = f_0(\Phi^S)\delta_{\alpha\beta} + \sum_N \xi_N(\Phi^s) \frac{\Phi^N_{\alpha\beta}}{M} + \mathcal{O}(\frac{\Phi^N}{M})^2 \quad (4)$$

where f_0 and ξ^N are functions of chiral singlet superfields, and M is the reduced Planck mass $= M_{Pl}/\sqrt{8\pi}$.

In equation (4), the contribution to the gauge kinetic function from Φ^N has to come through symmetric products of the adjoint representation of associated GUT group, since $f_{\alpha\beta}$ on the left side of (4) has such transformation property for the sake of gauge invariance. For $SO(10)$, one can have contributions to $f_{\alpha\beta}$ from all possible non-singlet irreducible representations to which Φ^N can belong :

$$(45 \times 45)_{symm} = 1 + 54 + 210 + 770$$

As an artifact of the expansion of the gauge kinetic function $f_{\alpha\beta}$ mentioned in equation (4), the gauge kinetic term (2nd term) in Lagrangian (equation (1) or equation (2)) can be recast in the following form

$$Re f_{\alpha\beta}(\phi) F_{\mu\nu}^\alpha F^{\beta\mu\nu} = \frac{\xi_N(\Phi^s)}{M_{Pl}} Tr(F_{\mu\nu} \Phi^N F^{\mu\nu}) \quad (5)$$

where $F_{\mu\nu}$, under unbroken $SO(10)$, contains $U(1)_Y$, $SU(2)$ and $SU(3)$ gauge fields.

Next, the kinetic energy terms are restored to the canonical form by rescaling the gauge superfields, by defining

$$F_{\mu\nu}^\alpha \rightarrow \hat{F}_{\mu\nu}^\alpha = \langle Re f_{\alpha\beta} \rangle^{\frac{1}{2}} F_{\mu\nu}^\beta \quad (6)$$

and

$$\lambda^\alpha \rightarrow \hat{\lambda}^\alpha = \langle Re f_{\alpha\beta} \rangle^{\frac{1}{2}} \lambda^\beta \quad (7)$$

Simultaneously, the gauge couplings are also rescaled (as a result of (4)):

$$g_\alpha(M_X) \langle Re f_{\alpha\beta} \rangle^{\frac{1}{2}} \delta_{\alpha\beta} = g_c(M_X) \quad (8)$$

where g_c is the universal coupling constant at the GUT scale. This shows clearly that the first consequence of a non-trivial gauge kinetic function is non-universality of the gauge couplings g_α at the GUT scale, if $\langle f_{\alpha\beta} \rangle$ carries a gauge index [9, 10, 31].

Once SUSY is broken by non-zero vev's of the F components of hidden sector chiral superfields, the coefficient of the last term in equation(2) is replaced by [9, 10]

$$\langle F_{\alpha\beta}^i \rangle = \mathcal{O}(m_{\frac{3}{2}} M) \quad (9)$$

where $m_{\frac{3}{2}} = \exp(-\frac{\langle G \rangle}{2})$ is the gravitino mass. Taking into account the rescaling of the gaugino fields (as stated earlier in equation (4) and (5)) in equation (6), the gaugino mass matrix can be written down as [9, 11]

$$M_\alpha(M_X)\delta_{\alpha\beta} = \sum_i \frac{\langle F_{\dot{\alpha}\dot{\beta}}^i \rangle}{2} \frac{\langle \partial f_{\alpha\beta}(\phi^{*i}) / \partial \phi^{*i}_{\dot{\alpha}\dot{\beta}} \rangle}{\langle \text{Re} f_{\alpha\beta} \rangle} \quad (10)$$

or

$$M_\alpha(M_X)\delta_{\alpha\beta} = \frac{1}{4} e^{-G/2} G^i ((G^{-1})_i^j) \frac{\langle \partial f_{\alpha\beta}^*(\phi^*) / \partial \phi^{*j} \rangle}{\langle \text{Re} f_{\alpha\beta} \rangle} \quad (11)$$

which demonstrates that the gaugino masses are non-universal at the GUT scale.

The underlying reason for this is the fact that $\langle f_{\alpha\beta} \rangle$ can be shown to acquire the form $f_\alpha \delta_{\alpha\beta}$, where the f_α 's are purely group theoretic factors, as we will see. On the contrary, if symmetry breaking occurs via gauge singlet fields only, one has $f_{\alpha\beta} = f_0 \delta_{\alpha\beta}$ from equation (4) and as a result, $\langle f_{\alpha\beta} \rangle = f_0$. Thus both gaugino masses and the gauge couplings are unified at the GUT scale, as can be seen from equations (8) and (10).

As mentioned earlier, we would like to calculate here, the f_α 's for Φ^N 's belonging to representations **54** and **770** through two possible breaking chains, namely, Pati-Salam gauge group $SU(2)_L \times SU(2)_R \times SU(4)_C$ (G_{224D} i.e with unbroken D -parity) and $SU(2) \times SO(7)$.

The results are tabulated in Table 1.

Breaking through G_{224} :

$SO(10)$ can be broken to $SU(2)_L \times SU(2)_R \times SU(4)_C$ (G_{224P}) using **54** and **770**-dimensional Higgs, such that D -parity remains intact. Using the $SO(10)$ relation, $(10 \times 10) = 1 + 45 + 54$ one can see that $\langle 54 \rangle$ can be expressed as a 10×10 diagonal traceless matrix. The branching of the $SO(10)$ representation 10 to G_{224} is

$10 \equiv (1,2,2) + (6,1,1)$. Thus the non-zero vev of 54 is

$$\langle 54 \rangle = \frac{v_{54}}{2\sqrt{15}} \text{diag}(3, 3, 3, 3, , -2, -2, -2, -2, -2, -2). \quad (12)$$

Since $(45 \times 45)_{\text{sym}} = 1 + 54 + 210 + 770$, and the branching of the $SO(10)$ representation 45 to G_{224} is

$$45 \equiv (15, 1, 1) + (1, 3, 1) + (1, 1, 3) + (6, 2, 2) \quad (13)$$

one can write the vev [13] of 770-dimensional Higgs as (45×45) diagonal matrix:

$$\langle 770 \rangle = \frac{v_{770}}{\sqrt{180}} \text{diag}(\underbrace{-4, \dots, -4}_{15}, \underbrace{-10, \dots, -10}_{3+3}, \underbrace{5, \dots, 5}_{24}) \quad (14)$$

In a intermediate scale (M_C), G_{224} is broken to SM gauge group. Thus the weak hypercharge Y generator can be expressed as a linear combination of the generators of $SU(2)_R \times SU(4)_C$ sharing the same quantum numbers. Then we can express the $U(1)_Y$ gaugino mass term as a linear combination of $SU(2)_R$ and $SU(4)_C$ gaugino masses.

We find the gaugino mass relation,

$$M_1 = \frac{2}{5} M_3 + \frac{3}{5} M_2 \quad (15)$$

54-dimensional representation:

Using 54-dimensional Higgs one gets $M_3 = -1$ and $M_2 = \frac{3}{2}$ and that leads to the gaugino mass term: $M_1 = \frac{1}{2}$. Therefore gaugino mass ratio is :

$$M_1 : M_2 : M_3 = (-\frac{1}{2}) : (-\frac{3}{2}) : 1 \quad (16)$$

770-dimensional representation:

Using 770-dimensional Higgs one gets $M_3 = 2$ and $M_2 = 5$ and that leads to the gaugino mass term: $M_1 = 3.8$. Therefore gaugino mass ratio is :

$$M_1 : M_2 : M_3 = 1.9 : 2.5 : 1 \quad (17)$$

Breaking through $SU(2) \times SO(7)$:

Again using the $SO(10)$ relation $(10 \times 10) = 1 + 45 + 54$ one can see that $\langle 54 \rangle$ can be expressed as a 10×10 diagonal traceless matrix. The branching of the $SO(10)$ representation 10 to $SU(2) \times SO(7)$ is

$$10 \equiv (3, 1) + (1, 7) \quad (18)$$

$$\langle 54 \rangle = \frac{v_{54}}{2\sqrt{15}} \text{diag}(7, 7, 7, -3, -3, -3, -3, -3, -3, -3). \quad (19)$$

Using the above vev of 54-dimensional higgs we get the gaugino mass ratio:

$$M_3 : M_2 : M_1 = 1 : (\frac{-14}{3}) : 1 \quad (20)$$

Since $(45 \times 45)_{sym} = 1 + 54 + 210 + 770$

The branching of the $SO(10)$ representation 45 to $SU(2) \times SO(7)$ is

$$45 \equiv (3, 1) + (1, 21) + (3, 7) \quad (21)$$

and one can write the vev of 770-dimensional Higgs as 45×45 diagonal matrix:

$$\langle 770 \rangle = \frac{v_{770}}{\sqrt{180}} \text{diag}(7, 7, 7, \underbrace{1, \dots, 1}_{21}, \underbrace{-2, \dots, -2}_{21}) \quad (22)$$

Using the above vev of 770-dimensional higgs we get the gaugino mass ratio:

$$M_3 : M_2 : M_1 = 1 : (14) : 1 \quad (23)$$

Table 1: High-scale gaugino mass ratios for representations of 54 and 770.

Representation	$M_3 : M_2 : M_1$ at M_{GUT}
1	1:1:1
54(i): $H \rightarrow SU(2) \times SO(7)$	1:(-14/3):1
54(ii): $H \rightarrow SU(4) \times SU(2) \times SU(2)$	1:(-3/2):(-1/2)
770(i): $H \rightarrow SU(2) \times SO(7)$	1:(14):1
770(ii): $H \rightarrow SU(4) \times SU(2) \times SU(2)$	1:(2.5):(1.9)

3 Low energy spectra, Consistency and Benchmark Points

Before we discuss the low-energy spectra for a wide region of the parameter space and their consistency for the non-universal points derived above, we study the evolution of these gaugino mass ratios with different RGE specifications and therefore the ratios obtained at the EWSB scale. As we know, the 1-loop RGE of the gaugino mass parameters doesn't involve the scalar masses [32], the ratios obtained with such RGE specifications are independent of the high scale values of the scalar masses namely, m_0 . If we also assume no radiative corrections (R.C) to the gaugino masses then the ratios obtained at the EWSB scale are also independent of the choice of the gaugino mass parameters at the high-scale. However, if one uses the 2-loop RGE in turn, the ratios of the gaugino masses at the EWSB scale decreases compared to the values obtained with one-loop RGE. Now, independently, the inclusion of R.C for the gaugino masses in the RGE, makes the M_3 lower, but makes M_1 , M_2 higher compared to the case of 1-loop RGE with no R.C. When, one uses both 2-loop RGE and R.C to the gauginos it is a competition between these two effects. As a whole, the

gaugino mass ratios at the EWSB scale crucially depend on the choice of RGE conditions and whether we take R.C into account. However, the dependence on the high-scale mass parameters m_0 and/or M_3 for any particular RGE condition is very feeble ¹.

We obtain the numerical results of our analysis using spectrum generator **SuSpect v2.3** [33]. We present in Table 2, the gaugino mass ratios at the EWSB scale for two different RGE conditions,

- 1-loop RGE with no R.C to the gaugino masses
- 2-loop RGE with R.C to the gaugino masses

where the 2-loop RGE + R.C to the gaugino masses have been obtained with $m_0 = M_3 = 500$ GeV, and $\tan\beta=10$.

Table 2: Low-scale (EWSB) gaugino mass ratios for representations 54 and 770.

Representation	$M_3 : M_2 : M_1$ 1-loop with No R.C	$M_3 : M_2 : M_1$ 2-loop with R.C
1 (mSUGRA)	1:0.27:0.13	1:0.35:0.19
54(i) : $H \rightarrow SU(2) \times SO(7)$	1:(-1.26):0.13	1:(-1.69):0.19
54(ii) : $H \rightarrow SU(4) \times SU(2) \times SU(2)$	1:(-0.40):(-0.06)	1:(-0.55):(-0.10)
770(i) : $H \rightarrow SU(2) \times SO(7)$	1:3.77:0.13	1:5.5:0.21
770(ii) : $H \rightarrow SU(4) \times SU(2) \times SU(2)$	1:0.67:0.24	1:0.91:0.37

Now we discuss the scan over the parameter space for the non-universal ratios obtained for different representations with different intermediate breaking chains. Here onwards, we will refer to these models as indicated in Table 1 or in Table 2. We study the numerical results by the spectrum generator **SuSpect** with the **pMSSM** option, as mentioned earlier. Following points are the broad specifications used in this RGE programme.

- In the running of parameters, two-loop renormalization group equations (RGE) have been used.
- Radiative corrections to the gaugino masses have been used.
- Full one-loop and the dominant two-loop corrections to the Higgs masses are incorporated.

¹In particular, with change in M_3 from 300-1000 GeV, with $m_0=1000$ GeV, the change in ratios is within 10%

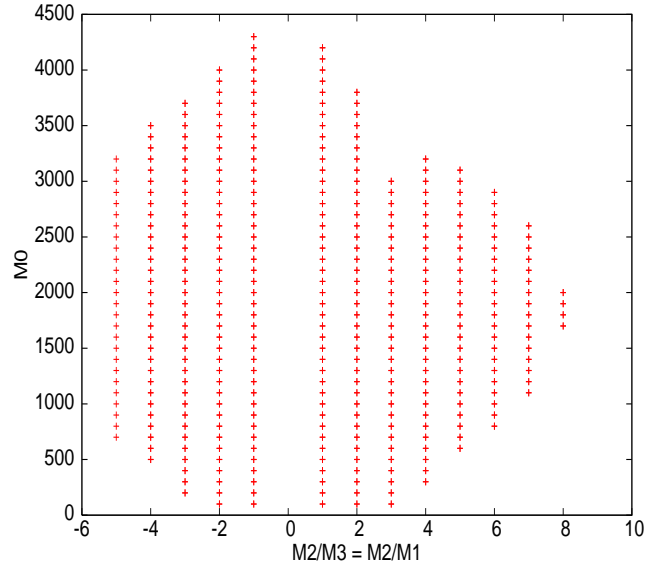


Figure 1: Variation of $M_2/M_1 = M_3/M_1$ with m_0 , for a generic study of the non-universal breaking pattern by the intermediate gauge group $SU(2) \times SO(7)$. Allowed regions by REWSB has been pointed out by red vertical lines. $M_1 = M_3 = 100$ GeV and $\tan \beta = 5$ is taken.

- Gauge coupling constant unification at the high scale have been ensured and the corresponding scale has been chosen as the 'high-scale' or 'GUT-scale' to start the running by RGE.
- Electroweak symmetry breaking at the 'default scale' $\sqrt{m_{t_L} m_{t_R}}$ has been set.
- We have used the strong coupling $\alpha_3(M_Z)^{\overline{MS}} = 0.1172$ for this calculation which is again the default option in **SuSpect**.
- Throughout the analysis we have assumed the top quark mass to be 171.4 GeV.
- All the scalar masses have been set to a universal value of m_0 and radiative electroweak symmetry breaking has been taken into account by setting high-scale higgs mass parameter $M_{H_u}^2 = M_{H_d}^2 = m_0^2$ and specifying $sgn(\mu)$, which has been taken to be positive throughout the analysis.
- All the trilinear couplings have been set to zero.
- Tachyonic modes for sfermions and other inconsistencies in RGE, like landau pole has been noted.
- As we work in a R -parity conserving scenario, stau-LSP regions have been identified.
- Consistency with low-energy FCNC constraints such as those from $b \rightarrow s\gamma$ has been noted for each combination of the parameter space. We have used a 3σ level constraint from $b \rightarrow s\gamma$ with the following limits[34].

$$2.77 \times 10^{-4} < Br(b \rightarrow s\gamma) < 4.33 \times 10^{-4}. \quad (24)$$

However, we must point out that we have pointed out all those regions as allowed where the value of $b \rightarrow s\gamma$ is lower than or within the constraint.

With these inputs, we scan the parameter space for a wide range of values of m_0 and M_3 ² for the non-universal gaugino mass ratios advocated above, as described below.

The ratios obtained for **54(ii)** at the high scale (see table 1) is actually the same as the one for the representation **24** in case of $SU(5)$ (see [9, 10, 11, 22]). This observation differs from the earlier result available in [12]. The low-energy spectrum and their consistency in this case (for **24**) have been well-studied [35] and without the inclusion of the intermediate

²Choice of M_3 automatically determines the values of M_1 and M_2 for a choice of non-universality

breaking scale in case of $SO(10)$, possibly this is difficult to distinguish from the one in $SU(5)$. However, choosing the intermediate scale different from the GUT scale, will change the gaugino mass ratios, which we do not address here. Hence, we do not illustrate the case of **54(ii)**.

However, we study the **54(i)** in details, where we see the generic pattern of breaking through $SU(2) \times SO(7)$, with $M_1 = M_3$ and $M_2 > M_3$, which also appears in the case of **770(i)**. We would like to point out that as the value of M_2 becomes larger and larger with respect to M_1 or M_3 , the region allowed by radiative electroweak symmetry breaking (REWSB) gets shrinked. It has been demonstrated in Figure 1, where we vary the $M_2/M_1 = M_3/M_1$ along the x-axis with m_0 varying along y-axis. It clearly shows that beyond $M_2/M_1 = M_3/M_1=8$, there is no allowed region where REWSB is satisfied. This is done for $M_3=100$ GeV and $\tan\beta=5$. The situation doesn't change too much with different choices of M_3 and $\tan\beta$. As in the case of **770(i)**, the ratio $M_2/M_1 = M_3/M_1=14$, we infer that no region at the low-scale is possible, which is allowed by REWSB.

Figure 2 shows the parameter space scan for the case of **54(i)** for $\tan\beta=5$ (left) and $\tan\beta=40$ (right). For the figure on the left hand side ($\tan\beta=5$), M_3 has been varied from 100 GeV to 2000 GeV, where m_0 has been varied from 100 GeV to 2000 GeV. Blue region is allowed by REWSB, whereas the yellow region is allowed by $b \rightarrow s\gamma$. The green shaded region is allowed by the constraint that no scalar can be tachyonic at the EWSB-scale. The whole region is allowed by stau-LSP constraint. Hence, only a very narrow region for small M_3 between 100 GeV to 200 GeV and high m_0 from 600 GeV to 2000 GeV is allowed by all constraints. In this region, we also calculate the relic density of the dark matter (DM) candidate (lightest neutralino) by `microOMEGA v2.0.7`[36] and point out regions allowed by the WMAP data[14] within 3σ limit

$$0.091 < \Omega_{CDM}h^2 < 0.128. \quad (25)$$

where $\Omega_{CDM}h^2$ is the dark matter relic density in units of the critical density and $h = 0.71 \pm 0.026$ is the Hubble constant in units of $100 \text{ Km s}^{-1} \text{ Mpc}^{-1}$. The region allowed by DM for **54(i)** with $\tan\beta=5$ (left) is noted as follows: m_0 within 1639 GeV to 1643 GeV for $M_3=200$ GeV; $m_0=1361$ -1372.5 GeV for $M_3=175$ GeV, $m_0=1220$ -1227 GeV for $M_3=150$ GeV, and $m_0=2690$ -2930 GeV for $M_3=125$ GeV. We also choose benchmark points (BP1, BP2 and BP3 as mentioned in Table 2 and 3) for our collider study from this dark matter allowed region.

The figure on the right hand side of Figure 2 is for **54(i)** with $\tan\beta=40$, as noted earlier. The first thing to point is that, the variation in $\tan\beta$ has made this figure markedly different

from the one with small $\tan\beta$. Here we have to scan a larger region in M_3 and m_0 plane, both varying from 100-6000 GeV to get a region allowed by the constraints. We note that the region allowed by REWSB shifts to higher M_3 value and comes with two distinct band, depicted in blue. The red region is allowed by the RGE constraints of having no tachyonic scalar mass or landau pole. The whole parameter space depicted here is allowed by $b \rightarrow s\gamma$ constraint, excepting for a small region at low M_3 , m_0 value within 100-300 GeV. No stau-LSP region occurs in this case. Hence, the region which is allowed by all constraints lies along the upper border of the narrow blue line (indicating REWSB). So, while it is a very narrow region which is allowed, at the same time it appears at very high value of M_3 , 2200 GeV onwards, and hence, the corresponding low-scale spectra, in particular the strongly interacting particles, namely, the gluino and the squarks will be too high to be in the reach of the LHC. So, for the time being, we postpone the study of the relic density constraint and also refrain from choosing any benchmark points from here for the sake of the collider study.

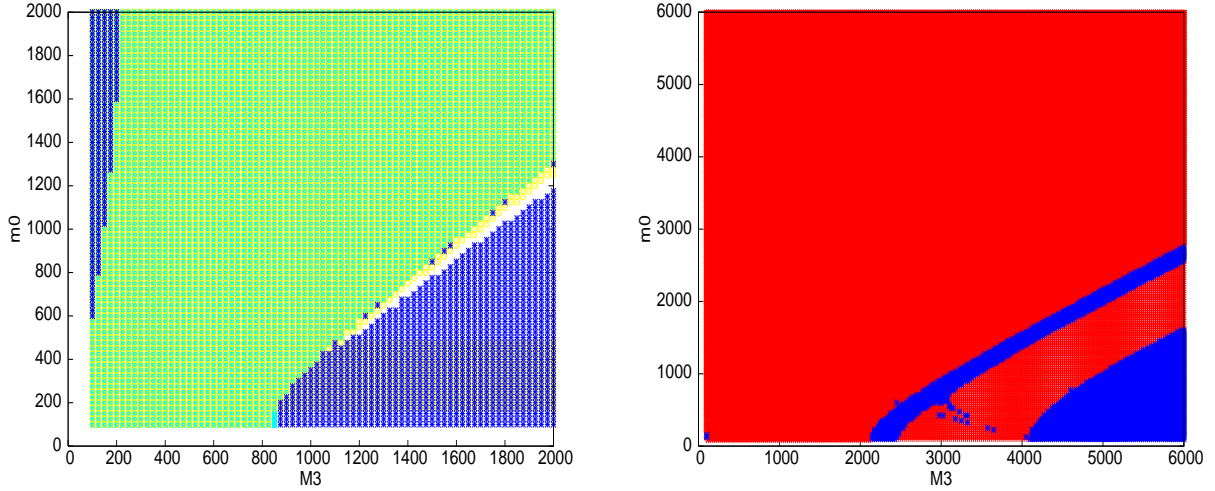


Figure 2: Parameter space allowed by various constraints for the representation **54** breaking through $SU(2) \times SO(7)$. **Figure on the left side:** $\tan\beta = 5$. *Allowed region lies in the left corner of the figure, depicted in blue.* **Figure on the right side:** $\tan\beta = 40$. *Allowed region lies along the upper border of the blue band from $M_3=2200$ GeV to 6000 GeV.*

In Figure 3, we depict the results of the scan in the $M_3 - m_0$ parameter space for the representation **770(ii)**, i.e. breaking through G_{224} . Once again, the figure on the left hand side is for $\tan\beta = 5$ and on the right hand side is for $\tan\beta = 40$. For the figure drawn for

$\tan\beta=5$, all the regions excepting for the discrete yellow spots are allowed by REWSB. The whole parameter space is also allowed by $b \rightarrow s\gamma$ and other RGE constraints, while the violate region at the bottom for $M_3=400-1100$ GeV with very small values of m_0 are disfavoured by the stau-LSP constraint. Hence, there is a large region of the parameter space which satisfies all the constraints and it is definitely within the reach of the LHC. We study the dark-matter constraints and our search is as follows: For $M_3=200$ GeV, the allowed range of m_0 spans around 200 GeV; for $M_3=400$ GeV, the allowed region is extremely narrow (because of the stau-LSP constraint) and is around $m_0=140$ GeV; for $M_3=600$ GeV, $m_0=300$ GeV is allowed and for $M_3=800$ GeV, the value of m_0 goes as high as 1100 GeV. We choose three benchmark points (BP4, BP5 and BP6, see Table 2 and 3) from here as well and study its collider signature.

The figure on the right hand side of Figure 3, with $\tan\beta=40$ is again quite different from the one with $\tan\beta=5$. Here, the region in yellow is allowed by REWSB. Excepting for a very narrow region at the left bottom corner spanning 100-200 GeV of M_3 or m_0 value, the whole region is under the $b \rightarrow s\gamma$ upper limit. The small m_0 region for $M_3=200-1400$ GeV, is disfavoured by stau-LSP. Hence, there exists a large region of parameter space, although shrunk a little compared to the case of $\tan\beta=5$, which is allowed by all the constraints for the study of dark-matter and collider search. The dark matter study in this case yields something special. We find almost all the regions to be underclosed with respect to the WMAP data. However, we choose a couple of benchmark points for the collider study.

Figure 4, shows similar parameter space scan for the case of mSUGRA, for $\tan\beta=5$ (left) and $\tan\beta=40$. These are presented to show the difference in patterns for the difference in high scale gaugino mass inputs. These have been studied very well and need not require illustrations. These also match with the earlier available results and hence show the robustness of our analysis. It is probably justified to mention that the whole region excepting for the violate band at small m_0 , which is disfavoured by stau-LSP, is allowed for $\tan\beta=5$, while a small region at high value of m_0 (1200-2000 GeV) and small value of M_3 (100-400 GeV) is disfavoured by REWSB constraint in addition to the stau-LSP region at the bottom in violate.

The benchmark points chosen from Figure 2 and 3, for collider simulation in context of the LHC, are presented in Table 3. Here we mention the high-scale values of the parameters, while the low-energy spectrum corresponding to these points have been mentioned in Table 4. These points as mentioned, satisfy the WMAP data for the cold dark matter relic density search. The corresponding values have also been tabulated. Only the points chosen for

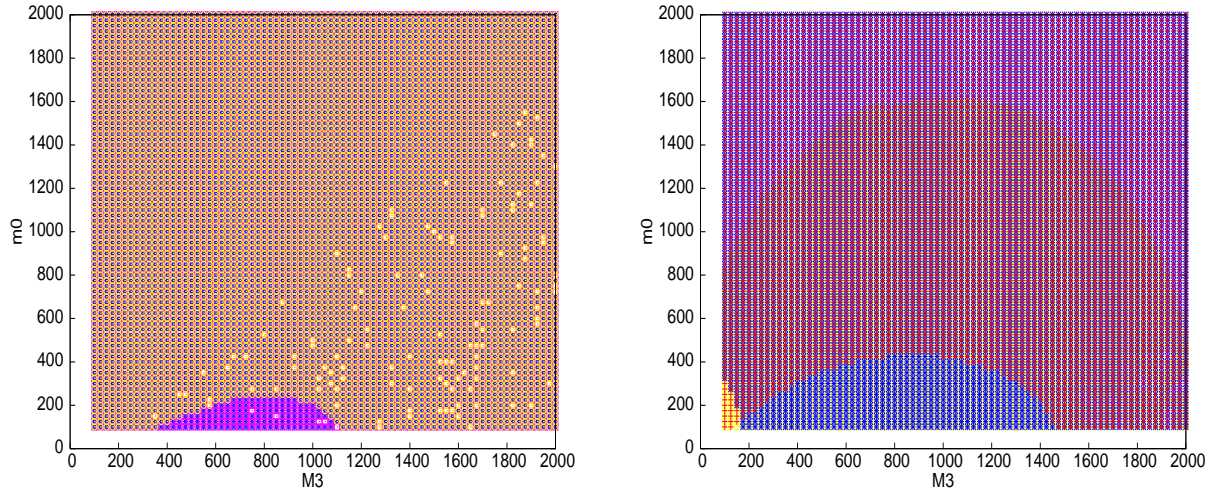


Figure 3: Parameter space allowed by various constraints for the representation **770** breaking through G_{224} . Figure on the left side: $\tan \beta = 5$. The whole region is allowed excepting for the yellow dots and the violate region at the middle bottom. Figure on the right side: $\tan \beta = 40$. The allowed region spans the whole M_3 excepting for very high values (1200-2000 GeV) and low values (100-400 GeV) of m_0 . It is shown in yellow.

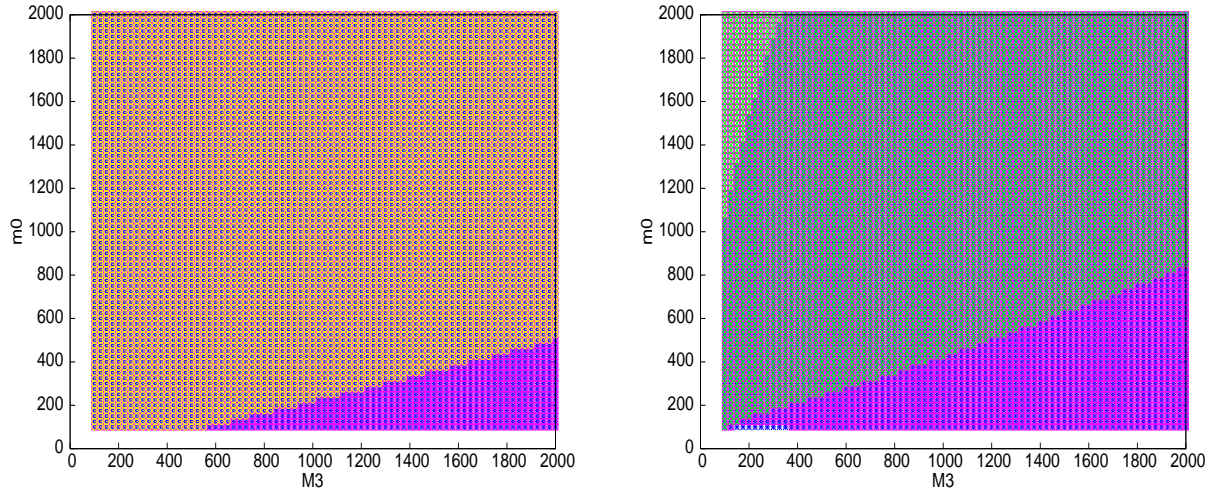


Figure 4: Parameter space allowed by various constraints for the **mSUGRA**. Figure on the left side: $\tan\beta = 5$. The whole region is allowed excepting for the violate region at low m_0 . Figure on the right side: $\tan\beta = 40$. The allowed region spans the whole M_3 excepting for very high values (1200-2000 GeV) at the top left corner and low values (100-600 GeV) of m_0 at the bottom of the figure.

770 – 224 for $\tan \beta = 40$ are all underclosed with respect to the WMAP data. The points chosen also obey the LEP bound, in particular for the Higgs mass [37].

Table 3: Benchmark Points: Models and High-Scale Parameters

Benchmark Points	Model	M_3	m_0	$\tan \beta$	$\Omega_{CDM} h^2$
BP1	54-27	125	2700	5	0.105
BP2	54-27	150	1225	5	0.105
BP3	54-27	200	1640	5	0.119
BP4	770-224	200	200	5	0.124
BP5	770-224	400	140	5	0.125
BP6	770-224	600	300	5	0.126
BP7	770-224	200	200	40	0.0002
BP8	770-224	400	700	40	0.0162

We tabulate the low-energy spectra of these benchmark points in the Table 4, as mentioned above. Here we note the gluino mass ($m_{\tilde{g}}$), average of the first two generation squark masses ($m_{\tilde{q}_{1,2}}$), average of the first two generation slepton masses ($m_{\tilde{l}_{1,2}}$), lighter stau mass ($m_{\tilde{\tau}_1}$), lighter stop ($m_{\tilde{t}_1}$), lightest neutralino ($m_{\tilde{\chi}_1^0}$), lighter chargino ($m_{\tilde{\chi}_1^\pm}$), 2nd lightest neutralino ($m_{\tilde{\chi}_2^0}$) as well as the value of μ . The composition (gaugino dominated, higgsino dominated or mixed) and the mass difference of the neutralinos and charginos get altered for different high-scale gaugino non-universality. Given the similar values of squark and gluino masses in different non-universal schemes (actually similar choice of M_3 and m_0), the electroweak gauginos become instrumental for a possible distinction in collider signature for different GUT-breaking schemes.

Table 4 : Low-energy spectra for the chosen benchmark points(BP)

Benchmark Points	$m_{\tilde{g}}$	$m_{\tilde{q}_{1,2}}$ $m_{\tilde{t}_1}$	$m_{\tilde{l}_{1,2}}$ $m_{\tilde{\tau}_1}$	$m_{\tilde{\chi}_1^0}$	$m_{\tilde{\chi}_1^\pm}$ $m_{\tilde{\chi}_2^0}$	μ
BP1	427.5	2687 1567.6	2702.5 2689	49.94	291.28 287.8	288.28
BP2	455.0	1286 695.54	1262.5 1221.46	53.16	154.72 151.68	150.35
BP3	590.93	1718 932.23	1689 1634.9	57.3	98.25 96.63	93.68
BP4	499.95	524 305.26	319.5 246.79	138.43	203.5 219.56	221.4
BP5	938.8	928 551.83	495 313.93	303.53	375.96 386.92	381.18
BP6	1368.48	1366 815.14	770.5 513.84	464.3	515.65 522.39	515.27
BP7	499.5	524.5 315	320 172.25	132.23	170.45 187.51	178.36
BP8	966.58	1145 699.06	857 597.87	246.73	262.11 269.58	261.83

4 Collider Simulation and Numerical Results

In this section, we would like to discuss the collider signature of the benchmark points motivated in the previous section.

In this section, we summarize the collider simulation procedure that has been adopted here and discuss the results obtained in context of the LHC. The spectrum generated by **SuSpect** v2.3 as described in the earlier section, at the benchmark points are fed into the event generator **Pythia** 6.4.16 [38] by **SLHA** interface [39] for the simulation of pp collision with centre of mass energy 14 TeV.

We have used **CTEQ5L** [40] parton distribution functions, the QCD renormalization and factorization scales being both set at the subprocess centre-of-mass energy $\sqrt{\hat{s}}$. All possible SUSY processes and decay chains consistent with conserved R -parity have been kept open. We have kept initial and final state radiations on. The effect of multiple interactions has been neglected. However, we take hadronization into account using the fragmentation functions

inbuilt in `Pythia`.

The final states studied here are :

- Opposite sign dilepton (*OSD*) : $(\ell^\pm \ell^\mp) + (\geq 2) \text{ jets} + E_{\cancel{T}}$
- Same sign dilepton (*SSD*) : $(\ell^\pm \ell^\pm) + (\geq 2) \text{ jets} + E_{\cancel{T}}$
- Tripleton ($3\ell + \text{jets}$): $3\ell + (\geq 2) \text{ jets} + E_{\cancel{T}}$
- Hadronically quiet tripleton (3ℓ): $3\ell + E_{\cancel{T}}$
- Inclusive 4-lepton (4ℓ): $4\ell + X + E_{\cancel{T}}$

where ℓ stands for final state electrons and or muons.

As defined in our earlier works [22], the absence of any jets with $E_T^{jet} \geq 100$ GeV qualifies the event as hadronically quiet. This avoids unnecessary removing of events alongwith jets originating from underlying events, pile up effects and ISR/FSR.

We have generated dominant SM events in `Pythia` for the same final states with same cuts. $t\bar{t}$ production gives the most serious backgrounds. We have multiplied the corresponding events in different channels by proper K -factor to obtain the usually noted NLO cross-section of $t\bar{t}$ [41]. The other sources of background includes WZ production, ZZ production etc. The contribution of each of these processes to the various final states are mentioned in the Table 6.

Before we mention the selection cuts, we would like to discuss the resolution effects of the detectors, specifically of the ECAL, HCAL and that of the muon chamber, which have been incorporated in our analysis. This is particularly important for reconstructing missing- E_T , which is a key variable for discovering physics beyond the standard model.

All the charged particles with transverse momentum, $p_T > 0.5$ GeV³ that are produced in a collider are detected due to strong B-field within a pseudorapidity range $|\eta| < 5$, excepting for the muons where the range is $|\eta| < 2.5$, due to the characteristics of the muon chamber. Experimentally, the main physics objects that are reconstructed in a collider, are categorized as follows:

- Isolated leptons identified from electrons and muons
- Hadronic Jets formed after identifying isolated leptons

³This is specifically for ATLAS, while for CMS, $p_T > 1$ GeV is used

- Unclustered Energy made of Calorimeter clusters with $p_T > 0.5$ GeV (ATLAS) and $|\eta| < 5$, that are not associated to any of the above types of high- E_T objects.

Isolated leptons are identified from electrons and muons with $p_T > 10$ GeV and $|\eta| < 2.5$. An isolated lepton should have lepton-lepton separation $\Delta R_{\ell\ell} \geq 0.2$, lepton-jet separation (jets with $E_T > 20$ GeV) $\Delta R_{\ell j} \geq 0.4$, the energy deposit $\sum E_T$ due to low- E_T hadron activity around a lepton within $\Delta R \leq 0.2$ of the lepton axis should be ≤ 10 GeV, where $\Delta R = \sqrt{\Delta\eta^2 + \Delta\phi^2}$ is the separation in pseudo rapidity and azimuthal angle plane. The smearing functions of isolated electrons, photons and muons are described below.

Jets are formed with all the final state particles after removing the isolated leptons from the list with PYCELL, an inbuilt cluster routine in **Pythia**. The detector is assumed to stretch within the pseudorapidity range $|\eta|$ from -5 to +5 and is segmented in 100 pseudorapidity (η) bins and 64 azimuthal (ϕ) bins. The minimum E_T of each cell is considered as 0.5 GeV, while the minimum E_T for a cell to act as a jet initiator is taken as 2 GeV. All the partons within $\Delta R=0.4$ from the jet initiator cell is considered for the jet formation and the minimum $\sum_{parton} E_T^{jet}$ for a collected cell to be considered as a jet is taken to be 20 GeV. We have used the smearing function and parameters for jets that are used in PYCELL in **Pythia**.

Now, as has been mentioned earlier, all the other final state particles, which are not isolated leptons and separated from jets by $\Delta R \geq 0.4$ are considered as unclustered objects. This clearly means all the particles (electron/photon/muon) with $0.5 < E_T < 10$ GeV and $|\eta| < 5$ (for muon-like track $|\eta| < 2.5$) and jets with $0.5 < E_T < 20$ GeV and $|\eta| < 5$, which are detected at the detector, are considered as unclustered energy and their resolution function have been considered separately and mentioned below.

- Electron/Photon Energy Resolution :

$$\sigma(E)/E = a/\sqrt{E} \oplus b \oplus c/E \quad (26)$$

Where,

$$\begin{array}{llll} a = 0.03 [\text{GeV}^{1/2}], & b = 0.005 \text{ \& } & c = 0.2 [\text{GeV}] & \text{for } |\eta| < 1.5 \\ = 0.055 & = 0.005 & = 0.6 & \text{for } 1.5 < |\eta| < 5 \end{array}$$

- Muon P_T Resolution :

$$\sigma(P_T)/P_T = a \quad \text{if } P_T < \xi \quad (27)$$

$$= a + b \log(P_T/\xi) \quad \text{if } P_T > \xi \quad (28)$$

Where,

$$\begin{aligned} a &= 0.008 & \& \ b &= 0.037 & \text{for } |\eta| < 1.5 \\ &= 0.02 & & &= 0.05 & \text{for } 1.5 < |\eta| < 2.5 \end{aligned}$$

- JET Energy Resolution :

$$\sigma(E_T)/E_T = a/\sqrt{E_T} \quad (29)$$

Where,

$$a = 0.55 \text{ [GeV}^{1/2}\text{]}, \text{ default value used in PYCELL.}$$

- Unclustered Energy Resolution :

$$\sigma(E_T) = \alpha \sqrt{\sum_i E_T^{(Unc.E)_i}} \quad (30)$$

Where, $\alpha \approx 0.55$. One should keep in mind that the x and y component of $E_T^{Unc.E}$ need to be smeared independently and by the same quantity.

Once we have identified the physics objects as described above, we vector sum the x and y component of the smeared momentum separately for isolated leptons, jets and unclustered energy to form visible $p_T = \sum p_x^2 + \sum p_y^2$ and identify the negative of the visible p_T as missing energy (\cancel{E}_T).

Finally the selection cuts that are used in our analysis are as follows:

- Missing transverse energy $\cancel{E}_T \geq 100 \text{ GeV}$.
- $p_T^\ell \geq 20 \text{ GeV}$ for all isolated leptons.
- $E_T^{jet} \geq 100 \text{ GeV}$ and $|\eta_{jet}| \leq 2.5$
- For the hadronically quiet trilepton events, and also for inclusive 4ℓ events, we have used in addition, invariant mass cut on the same flavour opposite sign lepton pair as $|M_Z - M_{\ell_+\ell_-}| \geq 10 \text{ GeV}$.

We have checked the hard scattering cross-sections of various production processes with CalcHEP [42]. All the final states with jets at the parton level have been checked against

the results available in [25]. The calculation of hadronically quiet trilepton rates have been checked against [43], in the appropriate limits.

The numerical results of the collider simulation at the benchmark points are presented in Table 5, while Table 6 contains the results in similar channels from SM background. While we see the results are markedly different from each other, we point out the difficulty in identifying the signal for BP1, BP5 and BP8 over background. We would like to remind, that all of these points are with very high gluino and squark masses.

The cross-sections are named as follows: σ_{OSD} for OSD, σ_{SSD} for SSD, $\sigma_{3\ell+jets}$ for $(3\ell + jets)$, $\sigma_{3\ell}$ for (3ℓ) and $\sigma_{4\ell}$ for inclusive 4 lepton events 4ℓ .

Table 5: Cross-sections (pb) at the chosen benchmark points

Benchmark Points	σ_{OSD}	σ_{SSD}	$\sigma_{3\ell+jets}$	$\sigma_{3\ell}$	$\sigma_{4\ell}$
BP1	0.01386	0.0010	0.00032	NULL	NULL
BP2	0.5443	0.19253	0.05953	0.044	0.0101
BP3	0.190	0.095	0.0347	0.0052	0.0050
BP4	0.822	0.16	0.08	0.0352	0.012
BP5	0.0878	0.0203	0.0151	0.00095	0.00277
BP6	0.021	0.0028	0.0049	0.00031	0.0014
BP7	0.502	0.1804	0.0475	0.0129	0.0045
BP8	0.0321	0.0142	0.005	0.00017	0.00048

Table 6: Event-rates (pb) after cuts from SM Background

Model Point	σ_{OSD}	σ_{SSD}	$\sigma_{3\ell+jets}$	$\sigma_{3\ell}$	$\sigma_{4\ell}$
$t\bar{t}$	2.2208	0.0307	0.0027	0.0717	0.0000
ZZ, WZ, ZH	0.0213	0.0005	0.0007	0.0328	0.0030
$\gamma\gamma, Z\gamma$	0.0297	0.0000	0.0000	0.0000	0.0000
Total	2.2718	0.0312	0.0035	0.1045	0.0030

5 Summary and Conclusions

We have derived non-universal gaugino mass ratios for the representation **54** and **770** for two breaking chains, namely, $SU(2) \times SO(7)$ and $SU(4)_C \times SU(2)_L \times SU(2)_R$ (G_{224}) in a $SO(10)$ SUSY-GUT scenario. We have assumed that the breaking of $SO(10)$ to the intermediate gauge group and the latter in turn to the SM gauge group takes place at the GUT scale itself. While we point out some mistakes in the earlier calculation, we derive some new

results on the gaugino mass ratios. We scan the parameter space with different constraints taken into account and point out the allowed region of the parameter space. We also study the dark matter constraint in these models and study collider simulation at some selected benchmark points in context of the LHC. The scans presented, have many interesting features that might help us in understanding the correlation between high-scale input and low-energy spectra. We must mention here that the study is limited by the assumption that the series of symmetry breaking occurs at the GUT scale itself. It is essentially a simplification, although we know that the ratios are bound to change with different choices of the intermediate scale. Within such a framework we have performed a collider study which is more illustrative than exhaustive. It nonetheless elicits some characteristics of the signature space for such high-scale ratios in context of the LHC.

After completing this study, we came across reference [44], where the issue of gaugino non-universality in the context of $SO(10)$ and $E(6)$ has been addressed. While we agree completely with the corrected gaugino mass ratios for G_{224} , we have in addition calculated, the ratios for $SU(2) \times SO(7)$. Furthermore, the low-energy particle spectra in different cases have been derived in a comparative manner, and the allowed regions of the parameter space consistent with low-energy and dark matter constraints are obtained in each case. In addition, we have predicted event-rates for both the breaking chains in a multichannel study pertinent to the LHC. The distinguishability of relative rates in different channels has also been explicitly demonstrated by us.

Acknowledgment: We thank Biswarup Mukhopadhyaya and Amitava Raychaudhuri for many useful suggestions. We thank Sanjoy Biswas and Nishita Desai for their technical help. We also acknowledge some very helpful comments from Sourav Roy. This work was partially supported by funding available from the Department of Atomic Energy, Government of India for the Regional Centre for Accelerator-based Particle Physics, Harish-Chandra Research Institute. Computational work for this study was partially carried out at the cluster computing facility of Harish-Chandra Research Institute (<http://cluster.mri.ernet.in>).

References

- [1] For reviews see for example, H. E. Haber and G. L. Kane, “The Search For Supersymmetry: Probing Physics Beyond The Standard Model,” Phys. Rept. **117**, 75 (1985).
- [2] S. Dawson, E. Eichten and C. Quigg, “Search For Supersymmetric Particles In Hadron - Hadron Collisions,” Phys. Rev. D **31**, 1581 (1985); X. Tata, “What is supersymmetry

and how do we find it?,” arXiv:hep-ph/9706307.

- [3] A. V. Gladyshev and D. I. Kazakov, “Supersymmetry and LHC,” arXiv:hep-ph/0606288.
- [4] S. P. Martin, “A supersymmetry primer,” arXiv:hep-ph/9709356 and in G. Kane (ed), Perspectives On Supersymmetry, *World Scientific* (1998); M. E. Peskin, “Supersymmetry in Elementary Particle Physics,” arXiv:0801.1928 [hep-ph].
- [5] T. Moroi and L. Randall, “Wino cold dark matter from anomaly-mediated SUSY breaking,” Nucl. Phys. B **570** (2000) 455 [arXiv:hep-ph/9906527]; M. E. Gomez and J. D. Vergados, “Cold dark matter detection in SUSY models at large $\tan(\beta)$,” Phys. Lett. B **512** (2001) 252 [arXiv:hep-ph/0012020].
- [6] P. Langacker, “Grand Unified Theories And Proton Decay,” Phys. Rept. **72** (1981) 185.

D. V. Nanopoulos and K. Tamvakis, “Susy Guts: 4 - Guts: 3,” Phys. Lett. B **113** (1982) 151; J. R. Ellis, D. V. Nanopoulos and S. Rudaz, “Guts 3: Susy Guts 2,” Nucl. Phys. B **202** (1982) 43; L. E. Ibanez and G. G. Ross, “SU(2)-L X U(1) Symmetry Breaking As A Radiative Effect Of Supersymmetry Breaking In Guts,” Phys. Lett. B **110** (1982) 215; N. Polonsky and A. Pomarol, “GUT effects in the soft supersymmetry breaking terms,” Phys. Rev. Lett. **73** (1994) 2292 [arXiv:hep-ph/9406224].
- [7] A. A. Anselm and A. A. Johansen, “Susy GUT With Automatic Doublet - Triplet Hierarchy,” Phys. Lett. B **200** (1988) 331; R. Hempfling, “Neutrino Masses and Mixing Angles in SUSY-GUT Theories with explicit R-Parity Breaking,” Nucl. Phys. B **478** (1996) 3 [arXiv:hep-ph/9511288].
- [8] L. Alvarez-Gaume, J. Polchinski and M. B. Wise, “Minimal Low-Energy Supergravity,” Nucl. Phys. B **221** (1983) 495; A. H. Chamseddine, R. Arnowitt and P. Nath, “Locally Supersymmetric Grand Unification,” Phys. Rev. Lett. **49**, 970 (1982).
- [9] J. R. Ellis, C. Kounnas and D. V. Nanopoulos, “No Scale Supersymmetric Guts,” Nucl. Phys. B **247**, 373 (1984); J. R. Ellis, K. Enqvist, D. V. Nanopoulos and K. Tamvakis, “Gaugino Masses And Grand Unification,” Phys. Lett. B **155**, 381 (1985).
- [10] M. Drees, “Phenomenological Consequences Of N=1 Supergravity Theories With Non-minimal Kinetic Energy Terms For Vector Superfields,” Phys. Lett. B **158**, 409 (1985).

- [11] A. Corsetti and P. Nath, “Gaugino mass nonuniversality and dark matter in SUGRA, strings and D brane models,” *Phys. Rev. D* **64**, 125010 (2001) [arXiv:hep-ph/0003186].
- [12] N. Chamoun, C. S. Huang, C. Liu and X. H. Wu, “Non-universal gaugino masses in supersymmetric SO(10),” *Nucl. Phys. B* **624**, 81 (2002) [arXiv:hep-ph/0110332].
- [13] J. Chakraborty and A. Raychaudhuri, “A note on dimension-5 operators in GUTs and their impact,” *Phys. Lett. B* **673** (2009) 57 [arXiv:0812.2783 [hep-ph]].
- [14] E. Komatsu *et al.* [WMAP Collaboration], “Five-Year Wilkinson Microwave Anisotropy Probe Observations:Cosmological Interpretation,” arXiv:0803.0547 [astro-ph].
- [15] A. Datta, A. Datta and M. K. Parida, “Signatures of non-universal soft breaking sfermion masses at hadron colliders,” *Phys. Lett. B* **431**, 347 (1998) [arXiv:hep-ph/9801242]; A. Datta, A. Datta, M. Drees and D. P. Roy, “Effects of SO(10) D-terms on SUSY signals at the Tevatron,” *Phys. Rev. D* **61**, 055003 (2000) [arXiv:hep-ph/9907444].
- [16] H. Baer, C. h. Chen, F. Paige and X. Tata, “Signals for Minimal Supergravity at the CERN Large Hadron Collider II: Multilepton Channels,” *Phys. Rev. D* **53**, 6241 (1996) [arXiv:hep-ph/9512383].
- [17] S. Khalil, “Non universal gaugino phases and the LSP relic density,” *Phys. Lett. B* **484**, 98 (2000) [arXiv:hep-ph/9910408]; S. Komine and M. Yamaguchi, “No-scale scenario with non-universal gaugino masses,” *Phys. Rev. D* **63**, 035005 (2001) [arXiv:hep-ph/0007327].
- [18] G. Anderson, H. Baer, C. h. Chen and X. Tata, “The reach of Fermilab Tevatron upgrades for SU(5) supergravity models with non-universal gaugino masses,” *Phys. Rev. D* **61**, 095005 (2000) [arXiv:hep-ph/9903370]; K. Huitu, Y. Kawamura, T. Kobayashi and K. Puolamaki, “Phenomenological constraints on SUSY SU(5) GUTs with non-universal gaugino masses,” *Phys. Rev. D* **61**, 035001 (2000) [arXiv:hep-ph/9903528]; K. Huitu, J. Laamanen, P. N. Pandita and S. Roy, “Phenomenology of non-universal gaugino masses in supersymmetric grand unified theories,” *Phys. Rev. D* **72**, 055013 (2005) [arXiv:hep-ph/0502100].
- [19] K. Choi and H. P. Nilles, “The gaugino code,” *JHEP* **0704**, 006 (2007) [arXiv:hep-ph/0702146].

- [20] S. I. Bityukov and N. V. Krasnikov, “Search for SUSY at LHC in jets + E(T)(miss) final states for the case of nonuniversal gaugino masses,” Phys. Lett. B **469**, 149 (1999) [Phys. Atom. Nucl. **64**, 1315 (2001 YAFIA,64,1391-1398.2001)] [arXiv:hep-ph/9907257]; S. I. Bityukov and N. V. Krasnikov, “The LHC (CMS) discovery potential for models with effective supersymmetry and nonuniversal gaugino masses,” Phys. Atom. Nucl. **65**, 1341 (2002) [Yad. Fiz. **65**, 1374 (2002)] [arXiv:hep-ph/0102179].
- [21] K. Huitu and J. Laamanen, “Relic density in non-universal gaugino mass models with SO(10) GUT symmetry,” arXiv:0901.0668 [hep-ph]; U. Chattopadhyay, D. Das and D. P. Roy, “Mixed Neutralino Dark Matter in Nonuniversal Gaugino Mass Models,” arXiv:0902.4568 [hep-ph].
- [22] S. Bhattacharya, A. Datta and B. Mukhopadhyaya, “Non-universal gaugino masses: a signal-based analysis for the Large Hadron Collider,” JHEP **0710** (2007) 080 [arXiv:0708.2427 [hep-ph]]; S. Bhattacharya, A. Datta and B. Mukhopadhyaya, “Non-universal gaugino and scalar masses, hadronically quiet trileptons and the Large Hadron Collider,” Phys. Rev. D **78** (2008) 115018 [arXiv:0809.2012 [hep-ph]].
- [23] P. Binetrui, G. L. Kane, B. D. Nelson, L. T. Wang and T. T. Wang, “Relating incomplete data and incomplete theory,” Phys. Rev. D **70**, 095006 (2004) [arXiv:hep-ph/0312248]; J. L. Bourjaily, G. L. Kane, P. Kumar and T. T. Wang, “Outside the mSUGRA box,” arXiv:hep-ph/0504170; G. L. Kane, P. Kumar, D. E. Morrissey and M. Toharia, “Connecting (supersymmetry) LHC measurements with high scale theories,” Phys. Rev. D **75**, 115018 (2007) [arXiv:hep-ph/0612287].
- [24] A. A. Affolder *et al.* [CDF Collaboration], “Search for gluinos and scalar quarks in $p\bar{p}$ collisions at $\sqrt{s} = 1.8$ TeV using the missing energy plus multijets signature,” Phys. Rev. Lett. **88**, 041801 (2002) [arXiv:hep-ex/0106001].
- [25] A. Datta, G. L. Kane and M. Toharia, “Is it SUSY?,” arXiv:hep-ph/0510204.
- [26] V. D. Barger, W. Y. Keung and R. J. N. Phillips, “Dimuons From Gauge Fermions Produced In P Anti-P Collisions,” Phys. Rev. Lett. **55**, 166 (1985); H. Baer, X. Tata and J. Woodside, “Gluino Cascade Decay Signatures At The Tevatron Collider,” Phys. Rev. D **41**, 906 (1990).

- [27] A. Datta, K. Kong and K. T. Matchev, “Discrimination of supersymmetry and universal extra dimensions at hadron colliders,” *Phys. Rev. D* **72**, 096006 (2005) [Erratum-*ibid.* *D* **72**, 119901 (2005)] [arXiv:hep-ph/0509246].
- [28] H. Baer, X. Tata and J. Woodside, “Multi - lepton signals from supersymmetry at hadron super colliders,” *Phys. Rev. D* **45**, 142 (1992); R. M. Barnett, J. F. Gunion and H. E. Haber, “Discovering supersymmetry with like sign dileptons,” *Phys. Lett. B* **315**, 349 (1993) [arXiv:hep-ph/9306204].
- [29] G. Duckeck *et al.* [ATLAS Collaboration]. “ATLAS computing: Technical design report,”
- [30] E. Cremmer, B. Julia, J. Scherk, P. van Nieuwenhuizen, S. Ferrara and L. Girardello, “Superhiggs Effect In Supergravity With General Scalar Interactions,” *Phys. Lett. B* **79**, 231 (1978); E. Cremmer, B. Julia, J. Scherk, S. Ferrara, L. Girardello and P. van Nieuwenhuizen, “Spontaneous Symmetry Breaking And Higgs Effect In Supergravity Without Cosmological Constant,” *Nucl. Phys. B* **147**, 105 (1979); E. Cremmer, S. Ferrara, L. Girardello and A. Van Proeyen, “Coupling Supersymmetric Yang-Mills Theories To Supergravity,” *Phys. Lett. B* **116**, 231 (1982); E. Cremmer, S. Ferrara, L. Girardello and A. Van Proeyen, “Yang-Mills Theories With Local Supersymmetry: Lagrangian, Transformation Laws And Superhiggs Effect,” *Nucl. Phys. B* **212**, 413 (1983).
- [31] C. T. Hill, “Are There Significant Gravitational Corrections To The Unification Scale?,” *Phys. Lett. B* **135**, 47 (1984); Q. Shafi and C. Wetterich, “Modification Of GUT Predictions In The Presence Of Spontaneous Compactification,” *Phys. Rev. Lett.* **52**, 875 (1984).
- [32] S. P. Martin and P. Ramond, “Sparticle spectrum constraints,” *Phys. Rev. D* **48**, 5365 (1993) [arXiv:hep-ph/9306314].
- [33] A. Djouadi, J. L. Kneur and G. Moultaka, “SuSpect: A Fortran code for the supersymmetric and Higgs particle spectrum in the MSSM,” *Comput. Phys. Commun.* **176**, 426 (2007) [arXiv:hep-ph/0211331].
- [34] S. Chen, *et al.*, CLEO Collaboration, *Phys. Rev. Lett.* **87**, 251807 (2001), hep-ex/0108032; P. Koppenburg *et al.* [Belle Collaboration], “An inclusive measurement of

- the photon energy spectrum in $b \rightarrow \bar{c} s$ gamma decays,” *Phys. Rev. Lett.* **93**, 061803 (2004); B. Aubert, et al., BaBar Collaboration, hep-ex/0207076.
- [35] S. F. King, J. P. Roberts and D. P. Roy, “Natural Dark Matter in SUSY GUTs with Non-universal Gaugino Masses,” *JHEP* **0710** (2007) 106 [arXiv:0705.4219 [hep-ph]]; K. Huitu, R. Kinnunen, J. Laamanen, S. Lehti, S. Roy and T. Salminen, “Search for Higgs Bosons in SUSY Cascades in CMS and Dark Matter with Non-universal Gaugino Masses,” *Eur. Phys. J. C* **58** (2008) 591 [arXiv:0808.3094 [hep-ph]].
 - [36] G. Belanger, F. Boudjema, A. Pukhov and A. Semenov, “micrOMEGAs2.0: A program to calculate the relic density of dark matter in a generic model,” *Comput. Phys. Commun.* **176**, 367 (2007) [arXiv:hep-ph/0607059].
 - [37] W. M. Yao *et al.* [Particle Data Group], “Review of particle physics,” *J. Phys. G* **33**, 1 (2006).
 - [38] T. Sjostrand, S. Mrenna and P. Skands, “PYTHIA 6.4 physics and manual,” *JHEP* **0605**, 026 (2006) [arXiv:hep-ph/0603175].
 - [39] P. Skands *et al.*, “SUSY Les Houches accord: Interfacing SUSY spectrum calculators, decay packages, and event generators,” *JHEP* **0407**, 036 (2004) [arXiv:hep-ph/0311123].
 - [40] H. L. Lai *et al.* [CTEQ Collaboration], “Global QCD analysis of parton structure of the nucleon: CTEQ5 parton distributions,” *Eur. Phys. J. C* **12**, 375 (2000) [arXiv:hep-ph/9903282].
 - [41] S. Moch and P. Uwer, “Theoretical status and prospects for top-quark pair production at hadron colliders,” *Phys. Rev. D* **78** (2008) 034003 [arXiv:0804.1476 [hep-ph]].
 - [42] A. Pukhov, “CalcHEP 3.2: MSSM, structure functions, event generation, batchs, and generation of matrix elements for other packages,” arXiv:hep-ph/0412191.
 - [43] H. Baer, C. H. Chen, F. Paige and X. Tata, “Trileptons from chargino - neutralino production at the CERN Large Hadron Collider,” *Phys. Rev. D* **50** (1994) 4508 [arXiv:hep-ph/9404212].
 - [44] S. P. Martin, “Non-universal gaugino masses from non-singlet F-terms in non-minimal unified models,” arXiv:0903.3568 [hep-ph].